

# Unusual Appearance and Presentation of Supratentorial Subependymoma in an Adult Patient


Ahmed K. Abdel-Aal<sup>1\*</sup>, Maysoon F. Hamed<sup>2</sup>, Nasser S. Al Naief<sup>3</sup>, Surjith Vattoth<sup>1</sup>, Asim Bag<sup>1</sup>

1. Department of Radiology, University of Alabama at Birmingham (UAB), Alabama, USA

2. Department of Anesthesiology, University of Alabama at Birmingham (UAB), Alabama, USA

3. Department of Pathology and Medicine, University of the Pacific, California, USA

\* **Correspondence:** Ahmed K. Abdel-Aal, M.D., Department of Radiology, University of Alabama at Birmingham (UAB), 619 19th Street South, Birmingham, AL 35249, USA

 [akamel@uabmc.edu](mailto:akamel@uabmc.edu)

Radiology Case. 2012 Aug; 6(8):8-16 :: DOI: 10.3941/jrcr.v6i8.999

## ABSTRACT

We report a case of a large, heterogeneously enhancing, pathologically proven, supratentorial subependymoma in a 31-year-old male patient presenting with headache, nausea and vomiting as well as gait disturbances. Although most supratentorial subependymomas have distinctive MR features, our case demonstrated imaging findings that made it indistinguishable from other more aggressive malignant supratentorial intraventricular lesions. It is of paramount importance to consider supratentorial subependymomas in the differential diagnosis of supratentorial lesions, even if their radiological features were atypical.

## CASE REPORT

### CASE REPORT

A 31-year old male patient presented with headache, nausea and vomiting, as well as gait disturbances and speech problems. The patient had no co-morbidities. MRI was performed prior to any surgical intervention on 1.5 Tesla scanners. The imaging protocol consisted of; Sagittal T1, axial T1, axial FLAIR and axial T2-weighted images, as well as, contrast-enhanced axial and coronal T1-weighted images. Axial diffusion weighted sequence and post contrast dynamic susceptibility contrast perfusion imaging (DSCI) were also obtained.

MRI revealed a large intraventricular lesion located in the frontal horn and body of the left lateral ventricle, extending through the foramen of Monroe into the third ventricle (Fig. 1,2). The lesion measured 5.1 x 5.3 x 5.8 cm. This large mass was lobulated with well defined margin. The mass was iso- to hypointense (compared to gray matter) on T1 weighted sequence and hyperintense on T2 and FLAIR weighted sequences. In both T1 and T2 weighted sequences, the mass

was heterogeneous. There was no increased T2 signal in the adjacent brain parenchyma to suggest extraventricular extension or infiltration.

The lesion showed heterogeneous enhancement on contrast-enhanced T1-weighted images (Fig. 3). There were also multiple signal voids on all sequences from multiple prominent intratumoral vessels indicating hypervascularity of the lesion (Fig. 1,2). There was no MR evidence of calcification or hemorrhage. There was moderate obstructive hydrocephalus of both lateral ventricles with a large posterior left lateral ventricular diverticulum projecting medially and inferiorly into the quadrigeminal cistern, producing mild mass effect on the tectum and vermis (Fig. 4). Additionally, there was no edema in the adjacent brain parenchyma or any signs that would indicate extraventricular extension of the lesion.

On diffusion weighted imaging (DWI), there was multiple areas of hyperintense foci (Fig 5a) associated with low apparent diffusion coefficient (ADC) value suggestive of multiple foci of dense cellularity (Fig 5b). The intratumoral ADC values of the areas of diffusion restriction were

compared with the contralateral normal appearing white matter (NAWM). In all these areas, the ratio of ADC value of the tumor to NAWM was less than 1. The ratio of ADCmin (the minimum ADC of the tumor) to ADC of contralateral NAWM was 0.91. These findings are suggestive of moderately increased cellularity.

On perfusion imaging, there were a few foci of very high cerebral blood volume (CBV) (Fig 6). Relative CBV (rCBV) was calculated as the ratio of CBV of the lesion divided by the CBV value of contralateral NAWM. rCBVmax (maximum CBV of the tumor divided by CBV of contralateral NAWM) was 3.918.

The patient underwent surgical resection of his large intraventricular mass. The tumor consisted of white to tan tissue, and the histomorphological examination revealed a moderately cellular glial neoplasm, characterized by clusters of small, round, monomorphic, cytologically bland cells exhibiting indistinct cytoplasmic borders and supported by fibrillary background. The nuclei were round to oval with bland looking chromatin and minimal pleomorphism; with only few scattered pleomorphic nuclei present (Fig. 7). There were multiple microcysts formation filled with faintly basophilic material and a few thick hyalinized vessels (Fig. 8). Perivascular pseudorosettes were not present. Rare mitotic figures were seen as well as focal geographic necrosis but endothelial proliferation was not evident. Immunohistochemical stains for glial fibrillary acidic protein (GFAP) was diffusely positive, while staining with MIB-1 (proliferative marker) reacted with approximately 0.8% of the tumor nuclei (Fig. 9). The final histopathological examination was consistent with subependymoma.

Following surgery the patient had improvement in his speech, with less misuse and placement of words, and was able to name two out of two objects. He was able to remember certain specific facts from the day before surgery and was noted to have no new neurologic deficits. Follow up MRI was performed one day after surgery and showed no residual tumor and no postoperative complication. The patient was cleared to participate safely in activities of daily living without any concerns of injury. A week after surgery, the patient had a CT scan which showed no interval development of hydrocephalus or other complication. The patient remained hemodynamically stable throughout his hospital stay.

## DISCUSSION

Subependymomas are rare benign gliomas with a prevalence of 0.4% in asymptomatic patients versus 0.7% in symptomatic patients [1] and have been more commonly reported in elderly males with a mean age of 39-59 years [2,3,4,5]. Although the histogenesis of these tumors is still uncertain, they correspond histologically to WHO grade I of glial tumor classification [6] which accounts for their likelihood to remain asymptomatic throughout life [7].

In 1945 Scheinker first described subependymoma as tumor of the fourth ventricle arising from the subependymal

glial layer surrounding the cerebral ventricles that was observed in a series of seven cases. These tumors are characterized by expansile growth that lacks an infiltrative pattern on histological examination [8,9].

These tumors arise more frequently in the fourth ventricle (50-60%), with the majority of the remainder occurring in the lateral ventricle (30-40%) [4,5]. In the lateral ventricle, subependymomas have an affinity to the anterior portions [10]. Small number of cases has been incidentally reported in the brain parenchyma [11], cerebellopontine angle [12], septum pellucidum and the third ventricle [13,14].

According to Maiuri and co-workers [7], the most important factor related to the presenting symptoms in subependymoma is the tumor location. Tumor size at presentation is directly related to tumor location, with tumors blocking CSF pathways (e.g., fourth ventricle, foramen of Monro) presenting with smaller dimensions than tumors not impeding CSF (e.g. atrium of lateral ventricle) [7]. Our patient however, presented with hydrocephalus and clinical symptoms described above, when his tumor was larger than 5 cm.

Although the exact histogenesis of subependymomas is still uncertain, they most likely arise from subependymal glial cells. Although most tumors are pure subependymomas, about 10% may present with an admixture of ependymoma and subependymoma. Such combined tumors are classified as mixed ependymoma/subependymoma and are graded based on the ependymoma component [4,6,13].

Histologically, subependymoma is characterized by the presence of clusters of round cells supported by a fibrillary background and exhibiting discrete cytoplasmic borders. Microcystic degeneration may be identified in some areas. Nuclear pleomorphism may be encountered but mitotic activity is uncommon. Vascular proliferation, necrosis, foci of mineralization, hemosiderin, and focally sclerotic vessel changes may also be seen [15]. Perivascular pseudorosettes or true ependymal rosettes are not usually observed in subependymomas but are rather characteristic of ependymomas, unless admixture of the two tumors is present.

The role of MIB-1 staining index (an important and well-recognized marker of cell proliferation) in the diagnosis of subependymoma is well-documented. Prayson and Suh [15] reviewed 14 cases of subependymomas and reported a MIB-1 index range of 0-1.4 (mean 0.3). Subependymomas are characterized by an extremely low mean MIB-1 labeling index when compared to myxopapillary ependymomas and low-grade ependymomas [16]. Histologically, subependymomas are graded as WHO grade I due to absent mitoses and extremely low MIB-1 index [16]. It is noteworthy to mention that our case demonstrated only 0.8% MIB-1 labeling index; further confirming the diagnosis. Although this is an extremely benign tumor, rarely they may have tumoral melanization [17], or may undergo rhabdomyosarcomatous differentiation [18] or sarcomatous transformation of vascular stromal elements [19].

The MR imaging features of supratentorial subependymomas seems to differ from infratentorial

subependymomas in most cases. The presence of calcification is one of the differentiating features. Lobato et al. [13] reported that six of 11 infratentorial and one of 11 supratentorial subependymomas had calcification while Silverstein and colleagues [20] reported no calcification on CT images of a lateral ventricular subependymoma. Chiechi and colleagues [21] described the presence of calcification in all six cases of fourth ventricular subependymomas and the absence of calcification in all 11 lateral ventricular subependymomas on CT images. We found no evidence of calcification on MR images in our patient with supratentorial subependymoma although CT scans, if obtained, would have been more sensitive.

The enhancement pattern of supratentorial subependymomas is different from infratentorial subependymomas in most cases. Supratentorial subependymomas tend to show minimal or no enhancement, while infratentorial subependymomas tend to enhance heterogeneously. Combined reports of 21 lateral ventricular subependymomas describe 16 (76%) cases as showing minimal or no enhancement [13,14,21-25], and 5 (24%) cases as showing heterogeneous enhancement [13,21,25,26]. Conversely, among 34 fourth ventricular subependymomas, only 5 (15%) cases showed minimal or no enhancement [2,21,24], whereas 29 (85%) cases showed heterogeneous enhancement [2,13,21,26,27]. Our case was among the exceptions that showed heterogeneous enhancement despite its supratentorial location.

Hoeffel et al [28] evaluated 8 patients with intracerebral and spinal subependymomas. One supratentorial tumor was heterogeneous and pathological correlation revealed regions of necrosis, calcification, tumor vascularity, microcystic and macrocystic changes accounting for this heterogeneity. Lindboe et al [12] reported a case of highly vascularized subependymoma of the septum pellucidum with acute hemorrhage in the tumor and surrounding brain parenchyma. In our case, the tumor was hypervascular as evidenced by presence of signal void on MR and hyalinized vessel on histology.

A thorough clinicopathological and radiographic evaluation is required to distinguish subependymoma from other supratentorial ventricular tumors including ependymomas, choroids plexus tumors, subependymal giant cell astrocytoma, neurocytoma, meningioma, astrocytoma and metastatic disease [29,30]. These tumors generally tend to be heterogeneous on T1, T2 and FLAIR sequences due to areas of hemorrhage, necrosis and calcification and most of them tend to enhance heterogeneously, making their MR features indistinguishable from our case.

Diffusion weighted imaging is a unique MRI sequence that detects water motion in the tissue microenvironment. In normal tissue, water motion is maximum in the extracellular compartment due to less hindrance. In highly cellular tumor, there is constriction of extracellular space due to too many cells in a given voxel. This restricts free water motion, which is detected by diffusion weighted imaging [31,32,33]. Diffusion characteristics of subependymoma are poorly

reported in literature. In our case, there was subtle diffusion restriction on diffusion imaging with minimum ADC value of  $753 \times 10^{-6} \text{ mm}^2/\text{s}$  secondary to moderately increased cellularity. Low ADC value secondary to increased cellularity is a feature of high grade tumors rather than low grade tumors (like subependymoma). In low grade tumors ADC value is usually higher than normal appearing white matter (varies from  $790-890 \times 10^{-6} \text{ mm}^2/\text{s}$ ).

Perfusion characteristic of subependymoma is also not well documented in literature. On perfusion imaging, there were multiple areas of high rCBV, higher than the contralateral NAWM. Although intratumoral neoangiogenesis is the most common cause of high rCBV in high grade tumors, in this particular tumor multiple intratumoral thick hyalinized vessels rather than neoangiogenesis was probably the explanation of higher rCBV.

The prognosis of a patient with an intraventricular subependymoma is good, with gross surgical resection being curative [6]. In symptomatic patients, total surgical resection is the goal of therapy [13], since these tumors are benign, grow by slow expansion, and are not infiltrative [3,5,20]. Knowing that a tumor is a subependymoma before resection may sway the neurosurgeon to operate in a difficult location because gross total resection can often be achieved without removing normal brain structures [13].

The differential diagnosis of supratentorial intraventricular subependymoma include; ependymoma, central neurocytoma, subependymal giant cell astrocytoma, choroid plexus papilloma and carcinoma, intraventricular meningioma and metastasis. Consideration of the tissue within and composing the ventricular lining and the clinical findings provide the means to limit the differential diagnosis when analyzing an intraventricular mass on an imaging study [10]. Ependymomas are typically calcified, are more common in children, are more common in the fourth ventricle, and show intense enhancement on contrast enhanced images. Subependymomas and central neurocytomas have an affinity for the anterior portion of the lateral ventricle, and the later commonly demonstrate a heterogeneous cystic appearance on cross sectional images. Subependymomas are more common in older adults, whereas central neurocytomas are more common before 40 years of age. Subependymal giant cell astrocytomas always lie near the foramen of Monro and are characterized by frequent calcification, intense enhancement on contrast enhanced studies, and the presence of other stigmata seen in tuberous sclerosis. When a mass is centered on the choroid plexus, a highly vascular tumor such as choroid plexus papilloma, choroid plexus carcinoma, meningioma, or metastasis should be suspected. The characteristic heavily lobulated appearance of a choroid plexus tumor favors this diagnosis over other possibilities, although it is not always possible to distinguish between the more common benign form, the choroid plexus papilloma, and the less common malignant counterpart, the choroid plexus carcinoma. By using clinical, demographic, and imaging findings, one can significantly limit the differential diagnosis for many of the most common supratentorial intraventricular neoplasms [10].

## TEACHING POINT

Most supratentorial subependymomas have characteristic appearance on MR imaging, being homogeneous with no or minimal enhancement, which differentiates them from other supratentorial intraventricular tumors and also from infratentorial subependymomas. However, the large size, high vascularity, heterogeneous enhancement and presence of symptoms, should not persuade the radiologist to exclude it from his differential diagnosis. It is of paramount importance to consider supratentorial subependymomas in the differential diagnosis of supratentorial lesions, even if their radiological features were atypical.

## REFERENCES

1. Matsumura A, Ahyai A, Hori A, Schaake T. Intracerebral subependymomas: clinical and neuropathological analyses with special reference to the possible existence of a less benign variant. *Acta Neurochir (Wien)*. 1989;96(1-2):15-25. PMID: 2929389
2. Jooma R, Torrens MJ, Bradshaw J, Brownell B. Subependymomas of the fourth ventricle: surgical treatment in 12 cases. *J Neurosurg*. 1985 Apr;62(4):508-512. PMID: 3973720
3. Lombardi D, Scheithauer BW, Meyer FB, et al. Symptomatic subependymoma: a clinicopathological and flowcytometric study. *J Neurosurg*. 1991 Oct;75(4):583-588. PMID: 1885976
4. Scheithauer BW. Symptomatic subependymoma: report of 21 cases with review of the literature. *J Neurosurg*. 1978 Nov;49(5):689-696. PMID: 712391
5. Nishio S, Morioka T, Mihara F, Fikui M. Subependymoma of the lateral ventricles. *Neurosurg Rev*. 2000 Jun;23(2):98-103. PMID: 10926103
6. Wiestler O, Schiffer D. Subependymoma. In: *Pathology and genetics of tumors of the nervous system*. 1st ed. Lyon, France, IARC, 2000;80-81.
7. Maiuri F, Gangemi M, Iaconetta G, Signorelli F, Del Basso De Caro M. Symptomatic subependymomas of the lateral ventricles. Report of eight cases. *Clin Neurol Neurosurg*. 1997 Feb;99(1):17-22. PMID: 9107462
8. Scheinker I. Subependymoma: A newly recognized tumor of subependymoma derivation. *J Neurosurg*. 1945;2:232-240.
9. Burger PC, Scheithauer BW. *Atlas of tumor pathology: tumors of the central nervous system*, 3rd series. Washington, DC: Armed Forces Institute of Pathology, 1994:133-136.
10. Koeller KK, Sandberg GD. From the Archives of the AFIP. Cerebral intraventricular neoplasms: radiologic-pathologic correlation. *RadioGraphics*. 2002 Nov-Dec;22(6):1473-1505. PMID: 12432118
11. Ragel BT, Osborn AG, Whang K, Townsend JJ, Jensen RL, Couldwell WT. Subependymomas: An analysis of clinical and imaging features. *Neurosurgery*. 2006 May;58(5):881-889. PMID: 16639322
12. Lindboe CF, Stolt-Nielsen A, Dale LG. Hemorrhage in a highly vascularized subependymoma of the septum pellucidum: case report. *Neurosurgery*. 1992 Oct;31(4):741-745. PMID: 1407461
13. Lobato R, Sarabia M, Castro S, et al. Symptomatic subependymoma: report of four new cases studied with computed tomography and review of the literature. *Neurosurgery*. 1986 Oct;19(4):594-598. PMID: 3785597
14. Yamasaki T, Kikuchi H, Higashi T, Yamabe H, Moritake K. Two surgically cured cases of subependymoma with emphasis on magnetic resonance imaging. *Surg Neurol*. 1990 May;33(5):329-335. PMID: 2330534
15. Prayson RA, Suh JH. Subependymomas: clinicopathologic study of 14 tumors, including comparative MIB-1 immunohistochemical analysis with other ependymal neoplasms. *Arch Pathol Lab Med*. 1999 Apr;123(4):306-9. PMID: 10320142
16. Jallo GI, Zagzag D, Epstein F. Intramedullary subependymoma of the spinal cord. *Neurosurgery*. 1996 Feb;38(2):251-257. PMID: 8869051
17. Rosenblum MK, Erlandson RA, Aleksic SN, Budzilovich GN: Melanotic ependymoma and subependymoma. *Am J Surg Pathol*. 1990 Aug;14(8):729-736. PMID: 2378394
18. Tomilson FH, Scheithauer BW, Kelly PJ, Forbes GS. Subependymoma with rhabdomyosarcomatous differentiation: report of a case and literature review. *Neurosurgery*. 1991 May;28(5):761-68. PMID: 1876259
19. Louis DN, Hedley-Whyte ET, Martuza RL. Sarcomatous proliferation of the vasculature in a subependymoma. *Acta Neuropathol*. 1989;78(3):332-35. PMID: 2763807
20. Silverstein JE, Lenchik L, Stanciu MG, Shimkin PM. MRI of intracranial subependymoma. *J Comput Assist Tomogr*. 1995 Mar-Apr;19(2):264-267. PMID: 7890853
21. Chiechi MV, Smirniotopoulos JG, Jones RV. Intracranial subependymoma: CT and MR imaging features in 24 cases. *AJR Am J Roentgenol*. 1995 Nov;165(5):1245-1250. PMID: 7572512
22. Vaquero J, Cabezudo JM, Nombela L. CT scan in subependymoma. *Br J Radiol*. 1983 Jun;56(666):425-427. PMID: 6850230
23. Kim DG, Han MH, Lee SH, et al. MRI of intracranial subependymoma: report of a case. *Neuroradiology*. 1993;35(3):185-186. PMID: 8459915
24. Morrison G, Sobel DF, Kelly DM, Norman D. Intraventricular mass lesions. *Radiology*. 1984 Nov;153(2):435-442. PMID: 6333046
25. Jelinek J, Smirniotopoulos JG, Parisi JE, Kanzer M. Lateral ventricular neoplasms of the brain: differential diagnosis based on clinical, CT, and MR findings. *AJNR Am J Neuroradiol*. 1990 Jul-Aug;11(4):567-74. PMID: 2349896
26. Stevens JM, Kendall BE, Love S. Radiological features of subependymoma with emphasis on computed tomography. *Neuroradiology*. 1984;26(3):223-228. PMID: 6738854
27. Swartz JD, Zimmerman RA, Bilaniuk LT. Computed tomography of intracranial ependymomas. *Radiology* 1982 Apr;143(1):97-101. PMID: 7063750
28. Hoeffel C, Boukobza M, Polivka M, et al. MR manifestations of subependymomas. *AJNR Am J Neuroradiol*. 1995 Nov-Dec;16(10):2121-2129. PMID: 8585504
29. Armington WG, Osborn AG, Cubberley DA, et al. Supratentorial ependymoma: CT appearance. *Radiology*. 1985 Nov;157(2):367-372. PMID: 4048443

30. Karamitopoulou E, Perentes E, Diamantis I, Maraziotis T. Ki-67 immunoreactivity in human central nervous system tumors: a study with MIB1 monoclonal antibody on archival material. *Acta Neuropathol.* 1994(1);87:47-54. PMID: 7511316
31. Norris DG, Niendorf T, Hoehn-Berlage M, et al. Incidence of apparent restricted diffusion in three different models of cerebral infarction. *Magn Reson Imaging.* 1994;12(8):1175-1182. PMID: 7854024
32. Verheul HB, Balazs R, Berkelbach van der Sprenkel JW, et al. Comparison of diffusion-weighted MRI with changes in cell volume in a rat model of brain injury. *NMR Biomed.* 1994 Mar;7(1-2):96-100. PMID: 8068532
33. Qiao M, Malisza KL, Del Bigio MR, Tuor UI. Transient hypoxia-ischemia in rats: changes in diffusion-sensitive MR imaging findings, extracellular space, and Na<sup>+</sup>-K<sup>+</sup>-adenosinetriphosphatase and cytochrome oxidase activity. *Radiology.* 2002 Apr;223(1):65-75. PMID: 11930049

FIGURES



**Figure 1:** 31 year old male with subependymoma. MRI Axial FLAIR image showing heterogeneous, hyperintense lesion in the left lateral ventricle (arrow), with moderate bilateral lateral ventricular hydrocephalus. Note the tiny signal void vessels in the lesion indicating high vascularity (arrowhead). MRI: 1.5 Tesla magnet, FLAIR (TE = 8000, TR = 147), axial, 5 mm slice.

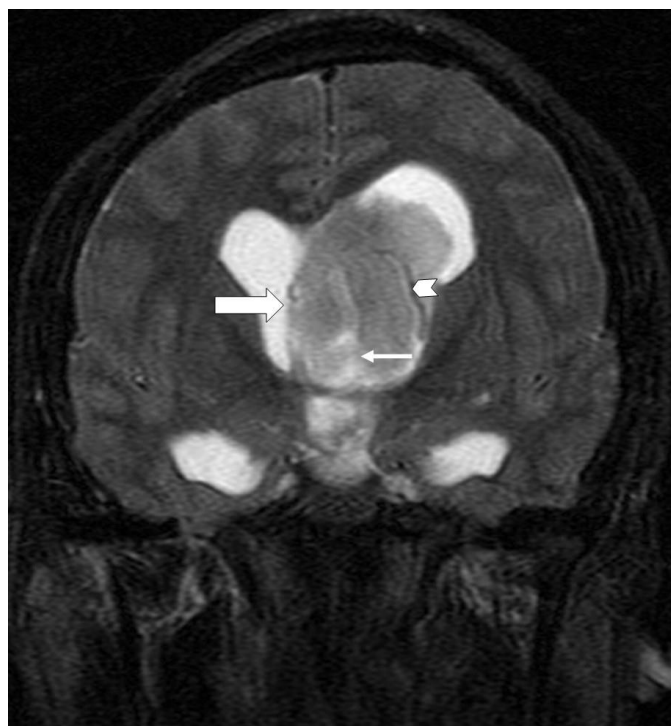


**Figure 2:** 31 year old male with subependymoma. MRI coronal T2-weighted image showing heterogeneous T2 hyperintense lesion in the left lateral ventricle extending into the third ventricle causing supratentorial hydrocephalus (arrow). Hyperintense cystic areas (small arrow) are also seen in the lesion. Note linear signal void vessel denoting high vascularity of the lesion (arrowhead). MRI: 1.5 Tesla magnet, T2 (TE 5000, TR 87), coronal, 5mm slice.

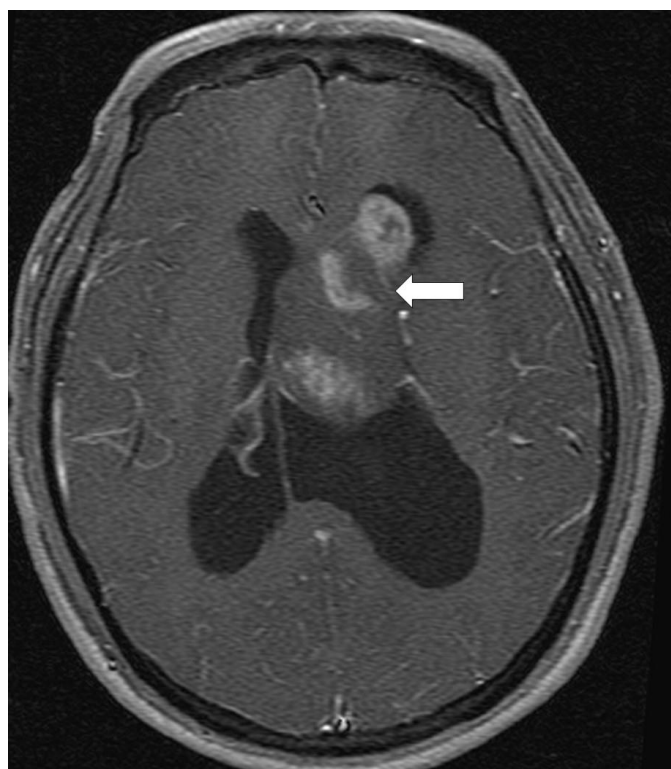


**Figure 3:** 31 year old male with subependymoma. MRI axial post-contrast T1-weighted image demonstrating heterogeneous enhancement of the lesion (arrow). MRI: 1.5 Tesla magnet, T1 with contrast (TE = 466, TR = 9), axial, gadolinium (Prohance), 15 ml.

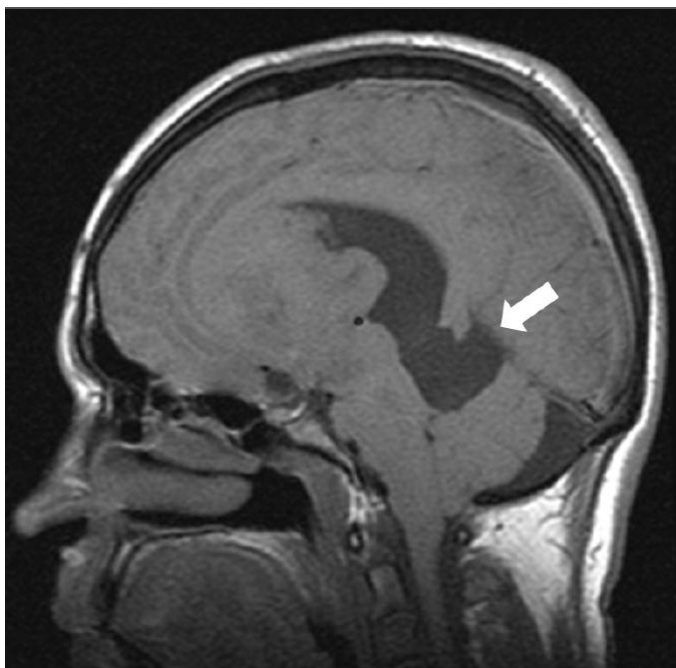


**Figure 4:** 31 year old male with subependymoma. MRI Axial T1 image showing large posterior left lateral ventricular diverticulum projecting medially and inferiorly into the quadrigeminal cistern, producing mass effect on the tectum and vermis (arrow). MRI: 1.5 Tesla magnet, T1 (TE =, TR =), axial, 5 mm slice.

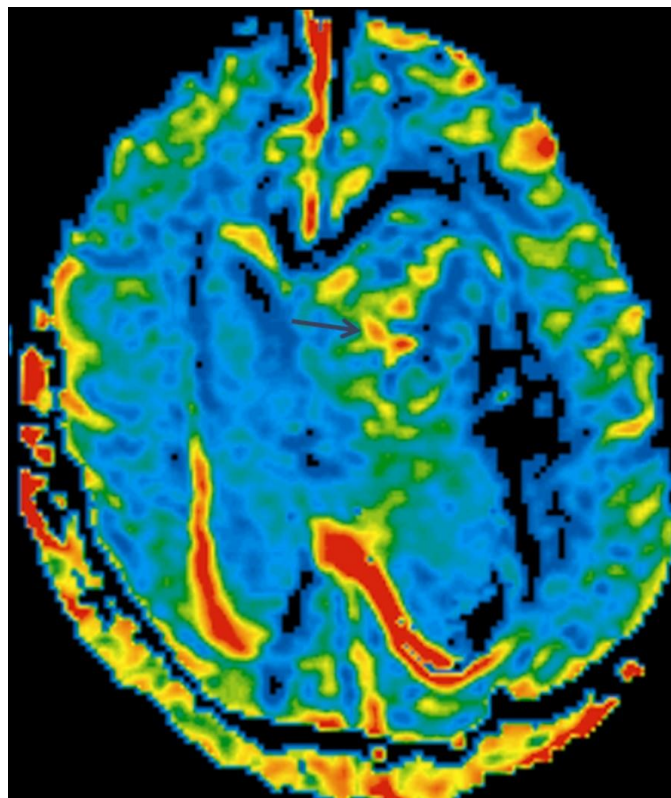


**Figure 6:** 31 year old male with subependymoma. MRI contrast enhanced dynamic susceptibility contrast perfusion image reveals multiple foci of high CBV (arrow) within the tumor. MRI: 1.5 Tesla magnet, axial GRE EPI (TE = 40, TR = 2262).



**Figure 5:** 31 year old male with subependymoma. MRI Diffusion weighted sequence. (a) DWI image shows focal areas of hyperintensity (arrow). (b) ADC map shows areas of low ADC values (arrow) corresponding to areas of DWI hyperintensity suggesting moderately hypercellular tumor. MRI: 1.5 Tesla magnet, DWI (TE = 110, TR = 12000, b=1000), ADC map, axial, 5mm slice.

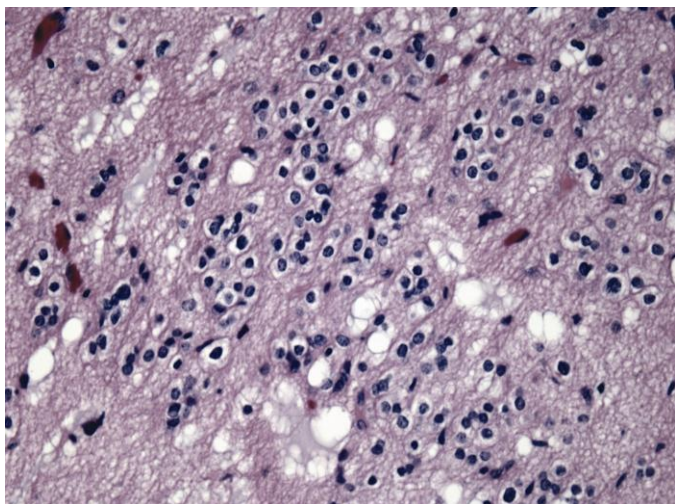


**Figure 7:** 31 year old male with subependymoma. Histomorphological examination of the tumor with Hematoxylin and eosin stain demonstrates clusters of round relatively monomorphous cells, supported by a fibrillary background and exhibiting discrete cytoplasmic borders. (original magnification X60).



**Figure 9:** 31 year old male with subependymoma. Histopathology with Immunoperoxidase staining for MIB-1. Immunohistochemistry staining of subependymoma with MIB-1 proliferative marker demonstrated positive labeling of approximately 0.8% of tumor cells (original magnification X 20).

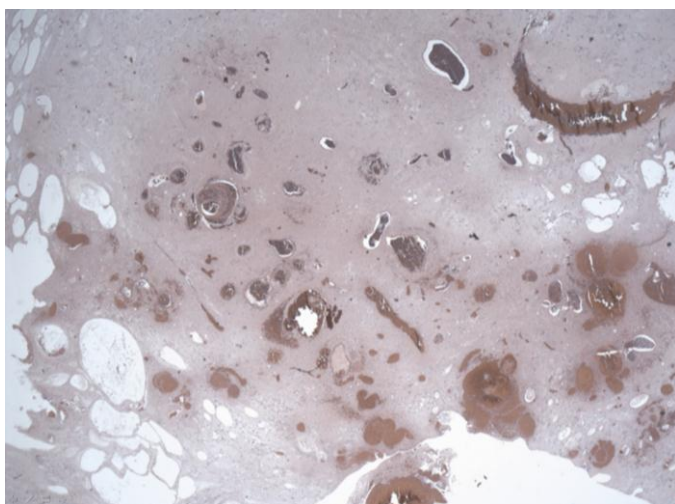


**Figure 8:** 31 year old male with subependymoma. Histopathology with Hematoxylin and eosin stain. The tumor also demonstrated vascular proliferation and necrosis. Sclerotic vessel changes were also focally appreciated (original magnification X40).

	Age	CT	MRI-T1	MRI-T2	contrast
<b>Supratentorial Subependymoma</b>	39-59	Iso- to hypoattenuated; hydrocephalus in 85% of cases, calcification in 31%, cysts in 18%, hemorrhage rare; focal enhancement	Hypointense at T1WI	Hyperintense at T2WI	Minimal or no enhancement
<b>Ependymoma</b>	Mean age 6 y for tumors in fourth ventricle and 18–24 y for supratentorial lesions	Usually isoattenuated; calcification in 40%–80% of lesions; enhancement usually intense but variable	Usually heterogeneous (calcification, hemorrhage, cysts); isointense at T1WI	Usually heterogeneous (calcification, hemorrhage, cysts); hyperintense at T2WI	Variable intense enhancement
<b>Central Neurocytoma</b>	20–40 y most common	Hyperattenuated; many small cystlike areas, calcification in 50% of cases	Hyperintense at T1WI	Solid portions hypointense and cysts hyperintense at T2WI	variable enhancement
<b>Subependymal Giant Cell Astrocytoma</b>	Children; Associated with tuberous sclerosis	Calcified nodule near foramen of Monro; intense enhancement	Hypointense at T1WI	Heterogeneously hyperintense at T2WI	intense enhancement
<b>Choroid Plexus Papilloma</b>	50% of patients <10 y for lateral ventricle tumors; fourth ventricular lesions seen in patients 0–50 y	Iso- to hyperattenuated, Lobulated mass typically centered in atria of lateral ventricle; calcification in 24% of cases; intense enhancement	Iso- to hypointense at T1WI; flow voids common	Variably hyperintense at T2WI; flow voids common	Intense enhancement
<b>Choroid Plexus carcinoma</b>	Infants and young children	Heterogeneous attenuation; Vasogenic edema	Heterogeneous intensity; Vasogenic edema	Heterogeneous intensity; Vasogenic edema	Intense heterogeneous enhancement
<b>Intraventricular Meningioma</b>	Adults 30–60 y most common	Hyperattenuated atrial mass; calcification in 50% of cases; intense enhancement	Iso- to hypointense at T1WI	Iso- to hyperintense at T2WI;	Intense enhancement
<b>Metastasis</b>	Adults more common	Iso- to hyperattenuated	Hypointense at T1WI	Hyperintense at T2WI	Intense enhancement

**Table 1:** Differential diagnosis table for supratentorial subependymoma



<b>Etiology</b>	Glial tumor
<b>Incidence</b>	0.4 % in asymptomatic patients 0.7% in symptomatic patients
<b>Gender ratio</b>	Slight male prevalence
<b>Age predilection</b>	Mean age of 39-59 years
<b>Risk factors</b>	None
<b>Treatment</b>	Surgical resection if symptomatic
<b>Prognosis</b>	WHO grade 1, good prognosis
<b>Findings on MR imaging</b>	Supratentorial: Well defined, small (except if symptomatic), noncalcified lesions with minimal or no enhancement Infratentorial: well defined, small heterogeneous lesions with calcification and heterogeneous enhancement.

**Table 2:** Summary table for supratentorial subependymoma

**ABBREVIATIONS**

ADC = Apparent diffusion coefficient  
 ADCmin = Minimum ADC of the tumor  
 CBV = Cerebral blood volume  
 DWI = Diffusion weighted imaging  
 GFAP = Glial fibrillary acidic protein  
 NAWM = Normal appearing white matter  
 rCBV = Relative CBV  
 rCBVmax = maximum CBV of the tumor divided by CBV of contralateral NAWM

**KEYWORDS**

subependymoma; supratentorial; intraventricular; tumor; adult; MRI

**Online access**

This publication is online available at:  
[www.radiologycases.com/index.php/radiologycases/article/view/999](http://www.radiologycases.com/index.php/radiologycases/article/view/999)

**Peer discussion**

Discuss this manuscript in our protected discussion forum at:  
[www.radiolopolis.com/forums/JRCR](http://www.radiolopolis.com/forums/JRCR)

**Interactivity**

This publication is available as an interactive article with scroll, window/level, magnify and more features.  
 Available online at [www.RadiologyCases.com](http://www.RadiologyCases.com)

Published by EduRad



[www.EduRad.org](http://www.EduRad.org)